Monte Carlo results for continuum percolation in low and high dimensions

N. Wagner,* I. Balberg, and D. Klein†
The Racah Institute of Physics, Hebrew University, Jerusalem 91904, Israel
(Received 28 December 2005; published 31 July 2006)

We report on Monte Carlo simulations of continuum percolation thresholds, by implementing highly efficient algorithms for very large samples. Our work, which includes percolation of hyperspheres, hypercubes, and boxes, in various dimensions, sizes, and shapes, has confirmed the expected dependence of the threshold on V_{ex}, the total excluded volume, and on B_c, the average number of bonds per site. We have further confirmed that $V_{ex}=B_c$, and that B_c is dependent on the objects shape, for which we offer a possible explanation. In particular we find that, counterintuitively, one can have $B_c<1$, as we have found for hyperspheres of dimension $\geqslant 12$. From our many results for differently sized hyperspheres, we were also able to derive the correlation length exponent ν solely from the behavior of the thresholds using finite-size scaling.

DOI: 10.1103/PhysRevE.74.011127 PACS number(s): 64.60.Ak, 02.50.Ng, 05.70.Jk, 64.60.Fr

I. INTRODUCTION

While many problems in random disordered media have been described by percolation theory, they have often been modeled through percolation on a lattice [1–3]. For many such systems this represents a useful simplification, one that has enabled the application of exact solution techniques [4] as well as efficient Monte Carlo simulations [5]. Specifically, if one is interested in the critical behavior, such modeling is a valid tool, since lattice and continuum systems are described by the same critical exponents [2]. Even the "nonuniversal" behavior of transport properties of systems that have diverging bond strengths (where the distribution arises naturally from the very nature of the continuum system [6]) can be modeled on lattices by imposing this divergent distribution on the lattice bonds [7]. Hence it is no wonder that lattice models have been used to describe many different continuum problems, such as flow in porous media [8], electrical conductivity in thin films [9] and doped semiconductors [10], elastic properties of composite materials [11], and gelation in polymers [12].

The percolation thresholds of such systems, however, cannot be adequately described by lattice models, since continuum and lattice percolation are not characterized by the same thresholds [13–16]. While there is a relationship between their thresholds, and certain continuum threshold values have been derived as limiting cases of lattice values [14], continuum percolation thresholds are, in general, described by different criteria than lattice thresholds. In fact, a comprehensive theory [15] predicting the thresholds of continuum percolation, using techniques of clustering theory in gases and liquids, does not require the assumption of any underlying lattice structure [16].

Indeed, while that density series expansion theory can predict, in principle, the percolation threshold of all continuum systems, in practice it does not always succeed, because it consists of a cluster-type expansion for the correlation function, containing many terms which are hard to calculate and which do not conveniently converge [16]. It is therefore generally necessary to perform simulations of different continuum systems, when one is interested in evaluating the threshold, for systems that contain objects of various sizes, shapes, and dimensions. Furthermore, as shown below, such simulations allow one to test the theory, both for cases where one can predict a definite value for the threshold, as well as for cases where one can establish upper or lower bounds from the terms. While substantial progress has been made in the study of high-dimensional percolation in lattices, we do not know of corresponding studies in the continuum. On lattices, the application of various renormalization group [17] and numerical [18–21] methods has enabled the derivation of quite accurate values of the threshold [18,19] and some critical exponents [20,21]. However, in spite of this, it was recently assessed [22] that "percolation in high dimensions is not understood," and this appears to be much more so in the case of percolation in the continuum. It is hoped that numerical simulations, as exhibited below, can take us to the frontier of high-dimensional continuum percolation and shed some light upon it.

In this work, we report on simulations that determine the percolation thresholds of three separate continuum systems: random hyperspheres, random hypercubes, and randomly oriented three-dimensional (3D) boxes. For the hyperspheres and hypercubes we check the dependence of the threshold on dimension, and for the 3D boxes we determine the dependence on the aspect ratio of the boxes. We shall relate these results to the exact theory, and to the other parameters that characterize the continuum threshold, i.e., $\langle V_{ex}\rangle$, the total average excluded volume, and B_c, the average number of bonds per site at the threshold.

The outline of this paper is then as follows. Section II contains a review of the various quantities used to characterize percolation thresholds in continuum systems. We describe our computations and present our results in Sec. III. In Sec. IV we use the results obtained from the thresholds of hyperspheres in order to determine the correlation length exponent, ν, for the various dimensions, by applying finite-size scaling [2], without the evaluation of any other quantities.

*Present address: Department of Chemistry, Ben-Gurion University of the Negev, Beer-Sheva, 84105, Israel.
†Present address: Oasis Capital Management, 1281 East Main St., Stamford, Connecticut 06902, USA.

Finally, we discuss and summarize the results obtained in this work in Sec. V.

II. PERCOLATION THRESHOLDS IN CONTINUUM SYSTEMS

In order to review the various ways by which one can characterize continuum percolation thresholds, we actually begin by looking at thresholds for lattice percolation [1,2]. Lattice percolation was originally introduced in two forms: site percolation, where the randomness is expressed by the occupation probability of the sites, and bond percolation, where the randomness is expressed by the occupation of the bonds between neighboring sites. These probabilities are usually denoted by p, and the corresponding percolation thresholds are usually denoted by p_c. The latter is simply the lowest value of p for which an infinite size cluster of connected sites or bonds exists [2].

In continuum percolation, we place N objects randomly throughout a *unit size* sample, and the threshold can be defined by N_c, the critical number of such objects (or by a proportional quantity). This model, while appearing as a site problem, can also be formulated as a bond problem [13,23]. The main difference in the definition lies in the fact that unlike p, which is bounded from above by unity, N, as such, does not well define a system: for example, it does not have an upper limit for the case of permeable (or soft core) objects. This lack of a natural normalization similarly prevents the comparison of the thresholds of differently sized systems. We shall see that the parameters we define subsequently to describe the continuum threshold do allow a comparison among different samples and various cases.

Unlike critical exponents, whose universal values are the same for different types of lattices in a given dimension, p_c depends on the lattice structure. It was first pointed out by Vyssotsky *et al.* [24], however, that for bond percolation zp_c is approximately a dimensional invariant, where z is the coordination number of the lattice, and that $zp_c \approx d/(d-1)$, where d is the dimensionality of the system. In the case of site percolation, zp_c is not an invariant, but Dalton *et al.* [25] showed that if one looks at zp_c for lattices of longer range interactions, i.e., lattices where sites connect with their nth nearest neighbors, zp_c tends to an asymptotic limit for $n \to \infty$ [4.5 in two dimensions (2D) and 2.7 in 3D].

A different invariant was found by Scher and Zallen [26] for site percolation. By attributing a circle (sphere) to each occupied site, when the centers are positioned on the lattice points, they found that fp_c (where f is the filling factor of the lattice), which is the critical area (volume) fraction of the system, is an approximate dimensional invariant [0.44 for 2D, 0.16 for 3D].

In fact, for continuum percolation, we shall see that the above two quantities are equivalent and also quasi-invariant. The application of the zp_c invariant to the continuum was first demonstrated by Shante and Kirkpatrick [14], who pointed out that zp_c is just the average number of intersections per site, and that the long range $n \to \infty$ limit described above corresponds to the case of interpenetrating continuum circles (spheres) distributed at random (since in the $n \to \infty$ limit the lattice constant tends to zero). Indeed, Monte Carlo simulations [13] for continuum circles and spheres have confirmed that B_c, the average number of "bonds" per site at threshold, gives the asymptotic values of zp_c in the $n \to \infty$ limit.

Alternatively, Scher and Zallen's invariant can be applied to the continuum, but there are several ways to do it. This is due to the overlapping nature of the continuum soft-core objects. Thus, one can look at the critical area (volume) fraction for continuum circles (spheres), σ_c (τ_c). On the other hand, one can use the *total* critical area (volume), $N_c s$ ($N_c v$) where s (v) is the area (volume) of an individual circle (sphere); this corresponds to the lattice parameter fp_c. These values are not equal, but one can easily show [14], using probability theory, that $\sigma_c = 1 - e^{N_c s}$ ($\tau_c = 1 - e^{N_c v}$). A careful look shows, however, that neither of these quantities can adequately describe the percolation threshold over the full range of continuum overlapping objects. For example, the percolation of 2D randomly oriented widthless sticks has been studied extensively for both the isotropic [13] and anisotropic cases [27]. Both N_c and B_c are well defined for this problem, yet both σ_c and $N_c s$ are always zero. Clearly, another parameter is needed. In passing, one should note that in the above expressions, as well as in our simulations, we assume that the sample is of a unit area or a unit volume, i.e., s and v are normalized area or volume of the permeable objects in the system with respect to the area or volume of the sample. Correspondingly, N_c is the critical number of objects in our sample, i.e., the objects' concentration at the threshold.

A criterion for the percolation threshold in the continuum was suggested by Balberg *et al.* [28] using the concept of excluded area (volume), first introduced by Onsager [29] in a different context. The excluded area (volume) of an object is defined as the area (volume) around this object into which the center of another similar object cannot enter without intersecting the first. Trivially, the excluded area (volume) of a circle (sphere) is simply the area (volume) of a circle (sphere) having double the radius. Thus the Scher and Zallen-like criterion, in this interpretation, suggests that the *total excluded area (volume) at threshold*, $A_{\mathrm{ex}} = N_c A$ ($V_{\mathrm{ex}} = N_c V$), is a dimensional invariant.

For a continuum system of randomly oriented objects, the excluded area (volume) of an object clearly depends on its orientation with respect to the intersecting objects. Therefore, one must compute the average excluded area (volume) for each object, $\langle A \rangle$ ($\langle V \rangle$), which, when multiplied by N_c, yields the total critical excluded area (volume), $\langle A_{\mathrm{ex}} \rangle = N_c \langle A \rangle$ ($\langle V_{\mathrm{ex}} \rangle = N_c \langle V \rangle$). The averaging is done by integrating over all possible orientations of the objects. By following this procedure one can compute [28,30,31] the excluded volume as a function of the aspect ratio for a system of randomly oriented capped cylinders. In particular, unlike the volume of the cylinder, which varies as Lr^2 (where L is the cylinder's length and r its radius), the excluded volume varies as $L^2 r$. The fact that V_{ex} is a quasi-invariant (see below), i.e., that $N_c \sim 1/L^2 r$, means, according to the above interpretation, that it is the average excluded volume of the objects, and not its volume, which determines the threshold. Simi-

larly, Charlaix *et al.* [32,33] have shown that the threshold of a randomly oriented system of disks follows their excluded volume, i.e., $N_c \sim 1/r^3$, and not their volume, which would yield $N_c \sim 1/r^2t$ (where r is the radius of the disk and t its thickness). Another extension of the study on 2D and 3D anistropically-oriented sticks [28,30] has shown that the functional dependence of the threshold on the system anisotropy can be predicted by assuming that the excluded area (volume) is an invariant of a system of objects of a given shape.

The actual values of the excluded area (volume) of the above systems show, however, that the total excluded area (volume) is not an exact invariant for a given dimension, but only a quasi-invariant for a given system [34]. Thus, in 2D, the total excluded area for systems of overlapping circles is 4.5, while for randomly oriented widthless sticks it is 3.6. In 3D, for overlapping spheres the total excluded volume is 2.8, while for the randomly aligned capped cylinders (of high L/r) it is 1.17. Similarly, for the lattice case introduced by Scher and Zallen, the total excluded areas and volumes are, respectively, 1.8 and 1.2. Thus a comprehensive theory for percolation thresholds cannot be based solely upon the concept of excluded area (volume). On the other hand, it seems clear that such a theory must reduce to the excluded area (volume) criterion for given systems.

In the search for such a comprehensive threshold theory, we note that the two quasi-invariants described above, B_c and A_{ex} (V_{ex}), are in fact equivalent for all cases of randomly placed permeable (potentially overlapping) objects in the continuum. This can be seen easily from the following argument: B_c, the average number of intersecting objects per given object at the threshold, is also the average number of object centers found within an excluded area (volume) of the object at this threshold. In a normalized system, the average number of objects at threshold within a given area (volume) is just N_c times this area (volume). Hence $B_c = N_c A = A_{\mathrm{ex}}$, ($B_c = N_c V = V_{\mathrm{ex}}$). This identity has also been confirmed numerically by Monte Carlo simulations [13,27,30] in which B_c and A_{ex} (V_{ex}) were computed differently.

A rigorous theory that predicts percolation thresholds, at least in principle, was proposed by Coniglio *et al.* [15] Using the density series expansion [35], they applied this tool to analyze the correlation function and the critical density for the case of percolation. Bug *et al.* [16] used this expansion to look at continuum soft-core percolation thresholds, demonstrating, in the corresponding cases, that to first order expansion the above theory reduces to the excluded volume criterion discussed above. On the other hand, they did not obtain any new numerical results using Congilio's theory. De Simone *et al.* [36] obtained numerical predictions for the threshold by using this expansion and the Percus-Yevick approximation. For the general case of soft-core, noninteracting, continuum percolation systems, Alon *et al.* [37] were able to show that Coniglio's expansion often yields an infinite number of terms which do not conveniently converge; hence, percolation thresholds cannot always be predicted using this exact theory. On the other hand, the expansion does yield upper and lower bounds for B_c in specific cases. For example, it can be shown [37] that $B_c \geqslant 1.1$ for 3D boxes, even for high aspect ratio. Also, in the high-dimensional limit, $B_c \to 1$ for the case of hypercubes; specifically, for hypercubes in 15 dimensions (15D) the expansion yields $B_c = 1.016$ to a good approximation. The latter examples underscore the fact that in very high dimensions, many of the higher order terms converge, yielding the above predictions. In general, however, one cannot assume that the expansion even converges; it is still necessary, therefore, to perform computer simulations or use other techniques to calculate percolation thresholds in the continuum.

Indeed, the higher-dimensional prediction for hypercubes is significant when one compares this case to higher-dimensional hyperspheres, for which no value or lower bound has been successfully predicted [37]. In fact, as we see below, our Monte Carlo results confirm that $B_c \geqslant 1$ for all higher-dimensional hypercubes, while for hyperspheres we find that B_c can be lower than unity for the very high dimensions. While Grassberger [19] has previously found for high-dimensional lattices that $V_{\mathrm{ex}} < 1$ for $d \geqslant 4$, the extension to the continuum is not obvious. This difference can be attributed to the fact that B_c and V_{ex} are expected to be equal only in the interpenetrating continuum limit but not in the lattices (see below). Our following findings of $B_c < 1$, while not in contradiction then with the finding on lattices, is rather unexpected. In fact it may be viewed as quite "counterintuitive" for the following reasons:

(1) In the infinite-dimensional limit, one expects the hypercontinuum to behave as a Bethe lattice [2] in the limit of large coordination number [2], i.e., $B_c = z/(z-1) \to 1$, so that it is larger than 1, though approaching 1 for $z \to \infty$.

(2) It was suggested by Zallen [1] that for percolation "the higher the dimensionality, the lower is the number of neighbors with which each site is in touch, and thus the closer its environment is to an average (i.e., mean field) environment." This can be interpreted as saying that for a high enough d, every site is an "average site." If there is a percolating path through such a system, each site, being an average site, must be connected to its environment since otherwise there is no connectivity in the system. Correspondingly, this intuitive picture implies that the average site has at least one bond to its environment, i.e., $B_c \geqslant 1$.

(3) Turning to the continuum, the $B_c \geqslant 1$ rule is consistent with the empirical prediction of Pike and Seager [16] that $B_c \approx (20)^{1/d}$ for random d-dimensional hyperspheres. The fact that it is apparently violated shows how little we still know about the continuum percolation threshold, despite the apparent simplicity of this concept and the many attempts made to describe it exactly. Moreover, the fact that even at very high dimensions the B_c values are around $B_c = 1$, yet they can also be above or below this value, depending on the shape of the objects, further suggests that the mean field approach is a good approximation as we go to high dimensions, but even there it is not an exact one.

III. COMPUTATIONS AND RESULTS

We ran many Monte Carlo simulations of continuum percolation in different dimensions, in order to compute the threshold, for three types of permeable objects: circles/spheres/hyperspheres, cubes/hypercubes, and boxes. In a

given simulation, all the objects were of the same size and shape and were randomly placed in a hypercontinuum of size unity. Intersecting objects were free to overlap. Hypercubes and boxes were fixed parallel to the system axes. The boxes, in 3D, consisted of two sides of equal length and a longer third side: the aspect ratio, which we varied in different samples, is defined as the ratio of the longer side to one of the equal sides. During the simulation, the long edge of each box was randomly placed parallel to one of the three axes [38].

Each simulation consisted of a random placing of such objects in the hypercontinuum, one at a time, until the percolation threshold was reached [38]. To do this, one must determine whether a given object intersects with any of the previously placed objects. In a direct approach, each jth object is checked against all $(j-1)$ previous objects. A more efficient algorithm [39] divides the hypercontinuum into "subhexes"; objects are then checked against other objects only within neighboring subhexes. The computation time for the direct approach is of the order N_c^2, where N_c is the critical number of objects at threshold; the time required for the subhex algorithm, for hypercubes and hyperboxes, is of the order of $3^d N_c$, where d is the dimension (for hyperspheres the subhex algorithm can be made even more efficient [39]). Therefore, the subhex algorithm was used for lower dimensions, allowing us to simulate very large samples efficiently. At very high dimensions, however, the factor 3^d becomes prohibitively high, so the direct approach was used.

With the intersections known, it was necessary to determine the clusters, until an "infinite" cluster [2] appeared (i.e., a cluster spanning the top and bottom boundaries) and the threshold was considered to be reached. The clustering was determined using our continuum variation [39,40] of the Hoshen-Kopenman algorithm [41].

Our results are presented in terms of the two parameters for continuum percolation described in Sec. II, V_{ex} and B_c. While these two quantities are theoretically equal (see below), they are computed differently in our simulations. V_{ex}, the total excluded volume, is just the product of N_c, by the (simply geometrically calculated [28]) average excluded volume of an object, V. For hyperspheres of radius r, this is just the volume of a hypersphere of radius $2r$; this volume in d dimensions can be expressed in terms of the Γ function, i.e.: $V=[\pi^{d/2}/\Gamma(d/2+1)](2r)^d$. (This can be shown from the general formula for a d-dimensional hypersphere: $V_d=V_{d-1}r\int_0^\pi \sin^d\theta\, d\theta$, where the definite integral yields $\Gamma[(d+1)/2]\Gamma(1/2)/\Gamma[(d+2)/2)]$, and the gamma function is given by $\Gamma(d+1)=d\Gamma(d)$, $\Gamma(1)=1$, and $\Gamma(1/2)=\sqrt{\pi}$). For even dimension, the above expression is simplified to: $V=\pi^{d/2}(2r)^d/(d/2)!$. Similarly, for hypercubes of edge e, the excluded volume is simply the volume of a hypercube of edge $2e$, $V=(2e)^d$. On the other hand, for hyperboxes, where the longer edges are not always parallel, the excluded volume is not proportional to the volume; for example, the volume of a 3D box of aspect ratio a is $v=ae^3$, while its excluded volume is given by (see the Appendix)

$$V=(2^3v/3)[1+(a+1)^2/2a]. \tag{1}$$

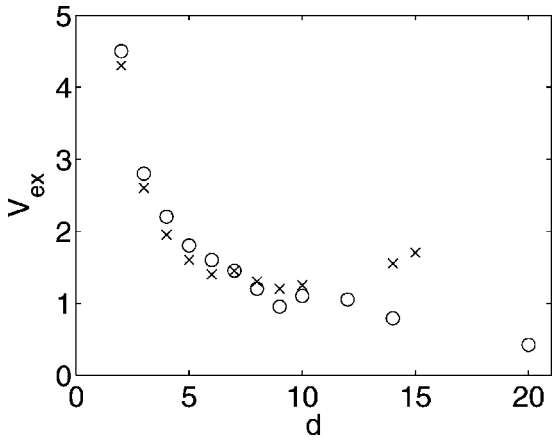

FIG. 1. The dependence of the total excluded volume on the system dimension d, for hyperspheres (○) and hypercubes (×). Shown here are our results for the largest samples that were used ($N_c=20\,000-30\,000$ for hyperspheres, $N_c=40\,000$ for hypercubes).

Alternatively, B_c is determined of course directly by computing the average number of intersections per object. Because of finite-size effects (an object near a boundary has fewer neighbors due to the cutoff of the sample), this averaging must be done only over those inner objects which do not intersect any boundary. At higher dimensions, where there are boundaries in all directions and the objects' diameters are simultaneously large (for values of N_c that are comparable to those used at lower dimensions), B_c is effectively computed over a very small sample. For example, for our largest hypersphere run in 14 dimensions (14D), the diameter was 0.45 (in a unit sample) and $N_c\approx 95\,000$; hence B_c was averaged over only $(1-0.45)^{14}\times 95\,000=22$ hyperspheres. The result for V_{ex} represents however the statistical effect of 95 000 hyperspheres, and finite-size effects can be properly taken into account (see below). Therefore, for large samples in low dimensions, B_c provides an additional value for the percolation threshold; for these cases, the proximity of B_c and V_{ex} gives us an estimate for the accuracy of our results. In general, however, V_{ex} is the better measure of the two; we therefore did not always compute B_c and most of our results will be presented in terms of V_{ex}.

We ran many samples of hyperspheres and hypercubes in 2D-10D, as well as hyperspheres in 12D, 14D, and 20D, and hypercubes in 14D and 15D. The results for our largest samples are presented in Fig. 1. The hypersphere results are averages over several (between 3 and 20) samples of $N_c=20\,000-30\,000$ [except for the 14D value that represents one run of $N_c\approx 95\,000$]; the hypercube values represent one run, each of $N_c\approx 40\,000$.

Our above results are consistent with previous Monte Carlo results for 2D circles [13]: 4.5; for 3D spheres [13,42]: 2.8; for four-dimensional (4D) hyperspheres [13]: 2.3; for 2D squares [13,43,44]: 4.4; for 3D cubes [44]: 2.6. In addition, our results are very close to previous theoretical approximations: lattice extrapolation [25] (see Sec. II), which yields 4.5 (2D) and 2.7 (3D) for spheres; series expansion of the mean cluster size [45], which yields 4.6 (2D) and 2.8 (3D) for spheres and 4.4 (2D) and 2.6 (3D) for cubes; and Pade' approximation of the mean cluster size [37,46], which yields

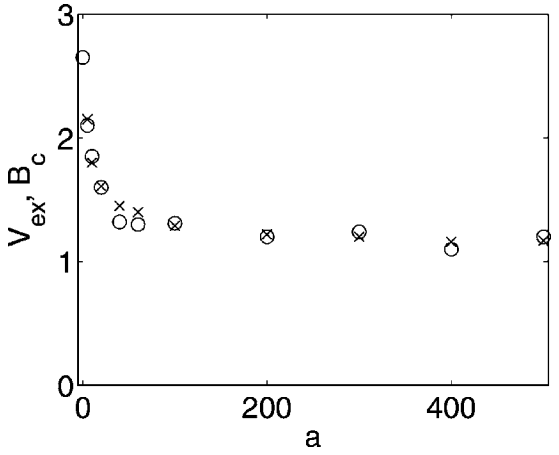

FIG. 2. The dependence of the total excluded volume, V_{ex} (○), and the average number of intersections per site, B_c (×), on the aspect ratio, a, for a system of 3D randomly-aligned boxes (N_c =40 000 with values averaged over ten runs).

2.8 (3D) for spheres and 4.7 (2D) and 2.6-2.7 (3D) for cubes.

We also looked at the thresholds of 3D boxes as a function of aspect ratio. Here it was appropriate (and feasible) to consider B_c as well as V_{ex} [using Eq. (1)], and the close proximity that we found bears this out. Our results are plotted in Fig. 2; each point represents the average value over ten samples of $N_c \approx 40\,000$.

We note then the similar behavior exhibited by the above cases, i.e., the decrease of the percolation threshold with increasing dimension or with increasing aspect ratio. However, a careful look shows this descent to be different for the three cases: for the boxes, the threshold seems to level off at about $V_{ex}=1.1$; for hyperspheres, the threshold descends below $V_{ex}=1$; for hypercubes, the threshold apparently levels off at some value about $V_{ex}=1.1$ (if we interpret the slight rise at high dimension to be a finite-size effect due to decreasing effective sample size; see below). In fact, these behaviors are consistent with the theoretical predictions of Drory *et al.* [37,38] summarized in Sec. II. It is significant that these authors have succeeded in showing that $V_{ex} \geqslant 1$ for hypercubes, but not for hyperspheres.

The fact that $V_{ex}=B_c<1$ for high-dimensional hyperspheres can be seen more clearly from the results presented in Fig. 3. Here, in order to take into account as much data as possible, we plot the largest samples in which both V_{ex} and B_c were computed (except for 14D and 20D, where only V_{ex} gave statistically meaningful results; see above) and averaged over ten runs (each of $N_c=10\,000-30\,000$). The error bars show the standard deviations within the samples; shown as well are various lattice values (from Kirkpatrick [47] and Grassberger [19]) for comparison. From our data, we can conclude a power-law behavior of the form of $V_{ex}=B_c \sim d^{-0.8}$. This, for the continuum, should replace then the old suggested relation [13] of the type $B_c \approx (20)^{1/d}$ (see Sec. II).

The question remains, however, if the low threshold at high dimensions is not merely a finite-size effect caused by the very large radii of the hyperspheres at these dimensions. For example, to obtain a threshold of about 30 000 hyperspheres, we use a very small radius of 0.0035 in 2D, but a very large radius of 0.245 in 14D. Even though finite-size scaling predicts larger thresholds for small samples (the true threshold being the lower bound of the computed values in the limit of infinite-sized sample; see Sec. IV), it is conceivable that an opposite effect takes place when the radius is too large, causing an artificially *low* threshold at *small* samples. To check the latter possibility we performed high-d simulations for several radii, and obtained the results shown in Fig. 4. Each point there represents the average V_{ex} value for ten runs and is shown with its standard deviation (the exception is our largest run in 14D, which represents one run only). It is clear from Fig. 4 that this possible finite size *opposite* effect does *not* take place, since the threshold consistently goes down for each dimension with the decrease of the radius (with a larger sample). Therefore, we conclude that normal finite-size scaling (lowering of the threshold with increasing sample size) does indeed hold also in our case, and

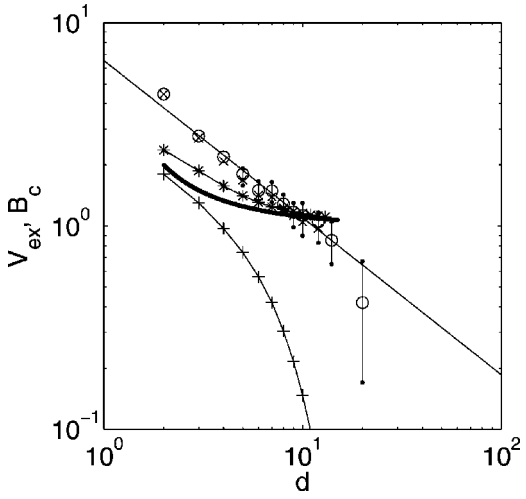

FIG. 3. The dependence of V_{ex} (○) and B_c (×) on the dimension d for hyperspheres. Shown here are our results for the largest hypersphere samples for which both V_{ex} and B_c were computed over ten runs ($N_c=10\,000-30\,000$). Also shown, for comparison, are lattice values of V_{ex} (+) for site percolation and of B_c(*) for bond percolation (taken from Refs. [19,47]), as well as the suggested invariant $d/(d-1)$ (bold solid line).

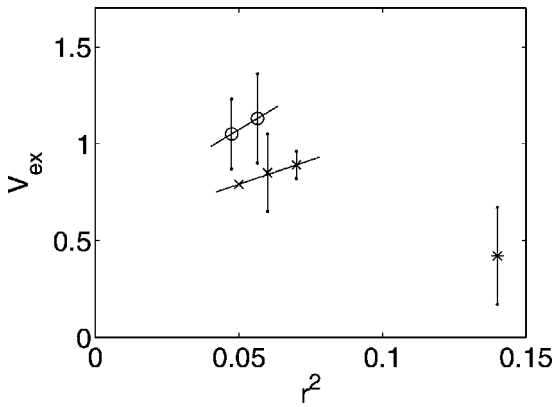

FIG. 4. The dependence of V_{ex} on the radius squared of hyperspheres of very high dimensions. These results are for $d=12$ (○), $d=14$ (×), and $d=20$(*).

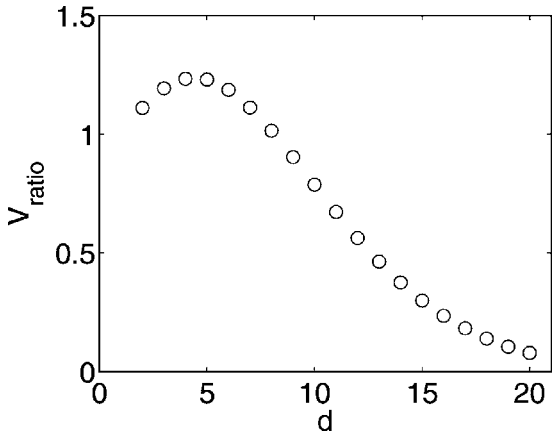

FIG. 5. The dependence of $V_{\text{ratio}}=V_{\bigcirc}/V_{\square}$ on the dimension d. $V_{\bigcirc}$ is the volume of a d-dimensional hypersphere, while $V_{\square}$ is the volume of an "effectively equivalent" hypercube.

thus our V_{ex} is clearly less than unity, since extrapolation to infinite size (zero radius) gives us even lower thresholds.

While the thresholds for hyperspheres are lower than for hypercubes in very high dimensions, the opposite is true at lower dimensions. To check this more accurately, we ran two very large simulations for 3D hypercubes. Our results, for V_{ex} and B_c, were obtained from averages of 100 runs each, with the error bars given by the standard deviation. For $N_c=10\,000$, we obtained $V_{\text{ex}}=B_c=2.68\pm0.11$; while for $N_c=100\,000$, $V_{\text{ex}}=B_c=2.63\pm0.05$. These are not only consistent with finite-size scaling, but the fact that V_{ex} equaled B_c within this accuracy underscores the reliability of the results, and also provides an excellent demonstration of the expected decrease of threshold with size, in continuum systems. It is clear therefore that V_{ex} for hypercubes is less than for hyperspheres ($V_{\text{ex}}=2.8$).

Why, as seen in Fig. 1, would hyperspheres have lower thresholds than hypercubes in higher dimensions while the reverse is true at lower dimensions? To answer this question, we compare the volume of a hypersphere, $V_{\bigcirc}$, with the volume of an "effectively equivalent" hypercube, $V_{\square}$, defined as the geometric mean of the volumes of the hypersphere's inscribed and circumscribed hypercubes. One would expect that the greater the volume, the larger the threshold for a given system. Figure 5 compares these two volumes as a function of dimension; at about $d=6$, $V_{\square}$ "overtakes" $V_{\bigcirc}$, which is roughly consistent with our Monte Carlo threshold results (see Fig. 1).

In fact, Alon [37,46] has suggested a heuristic argument to explain percolation thresholds. By looking at the "pointedness" of objects, he has predicted the thresholds for 3D spheres, $B_c=2.8$, and cubes, $B_c=2.6$. Our results are consistent with these predictions.

IV. FINITE-SIZE SCALING AND THE CORRELATION-LENGTH EXPONENT

So far we have dealt exclusively with percolation thresholds, which, unlike critical exponents, do not obey universality. Therefore, the studies of percolation thresholds and the percolation exponents are generally not related. However, in this section we shall obtain the correlation length critical exponent, ν, purely from calculations of the threshold, without calculating any of the critical quantities themselves.

The correlation length, ξ, of a given percolation network is defined [2] as its average connectivity distance, or the average distance of two sites belonging to the same cluster. It can be calculated by computing the average size of the finite clusters. The correlation length diverges, as the threshold is approached, with the exponent ν.

For finite samples at threshold, the correlation length is longer than the sample size and this affects the observed percolation threshold. The true threshold, which is defined in theory only for an infinite sample, is distinct from the observed values. Their average, however, converges to the "true" p_c value with the increase of the sample size. The above quantities can be related using the following two equations [2]:

$$p_{\text{av}} - p_{\text{c}} \propto L^{-1/\nu} \tag{2}$$

and

$$\Delta p_0 \equiv \sqrt{\langle p_0^2\rangle - \langle p_0\rangle^2} \propto L^{-1/\nu}. \tag{3}$$

Equation (2) refers to the fact that even though the onset of percolation p is expected to shift towards lower p values for a finite sample, the average observed percolation threshold, p_{av}, will be higher than p, and will differ from the true threshold by an amount which varies inversely with linear system size to the power $1/\nu$. Thus, in the infinite sample limit, $p_{\text{av}}\rightarrow p_c$.

Equation (3) refers to an additional feature of the observed threshold, namely, that the deviation of observed percolation threshold values p_0 from their average value, $p_{\text{av}}=\langle p_0\rangle$, also diminishes with increasing sample size, with the same dependence. When we use the corresponding ΔB_c or ΔV_c (rather than the Δp_0 used for lattices) we also obtain the same behavior. This deviation can be measured by using the standard deviation (as we did) or any other well-defined measure. Thus, by computing percolation thresholds many times for samples of many sizes, one can simultaneously obtain both the true value of p_c and the critical exponent ν.

Levinshtein *et al.* [48] first introduced Eq. (3), and used it to obtain ν for lattices in 2D ($\nu=1.33\pm0.04$) and 3D ($\nu=0.9\pm0.05$). To obtain these values, they performed thousands of runs for variously sized lattices. Stauffer and Aharony [2] similarly noted the large number of runs needed to obtain reasonable values for ν using Eq. (3), while a smaller number of runs is needed in order to obtain good values of ν from Eq. (2).

Our experience for the continuum has been different. We used our data for percolation thresholds to compute the value of ν, for 2D-10D, using Eq. (3). For each dimension we have looked at ten different sample sizes, for which we have computed both V_{ex} and B_c and their standard deviations, for ten different runs. We have used a variation of Eq. (3):

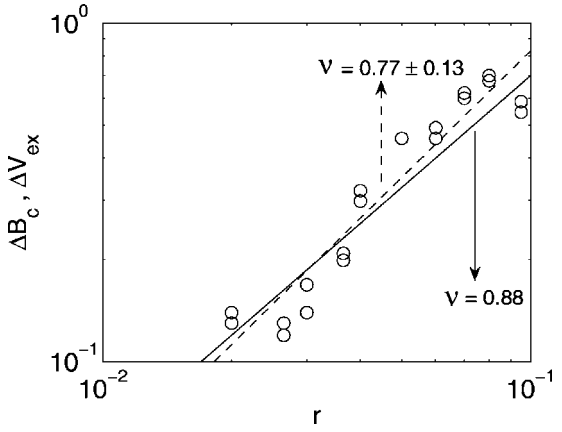

FIG. 6. Representative plot of the standard deviations of B_c and V_{ex} vs the hypersphere's radius r. Shown here are the results for 3D systems, from ten different runs, each for ten different sample sizes. We obtained the critical exponent ν by using a least-squares fit (dashed line) for the determination of the slope of the log-log plot, and then taking its reciprocal value. For comparison we show the expected (solid) line based on the accurate value that was obtained for lattices.

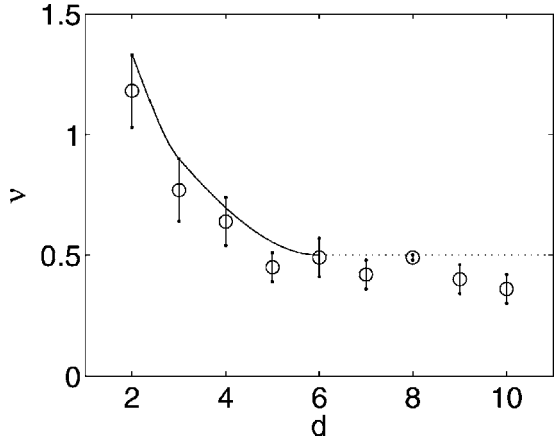

FIG. 7. The ν values (shown here with their confidence limits) vs the dimension d, as determined by least-squares fit from finite-size scaling. The solid curve shows the values presented in Ref. [49] for lattices, and the dotted line shows the prediction of mean-field behavior (Ref. [2]).

$$\sqrt{\langle p_0^2\rangle - \langle p_0\rangle^2} \propto r^{1/\nu}, \tag{4}$$

where r is the radius of the corresponding hypersphere. Equation (4), of course, takes into account the fact that a small radius is equivalent to a larger L. By plotting the standard deviations as a function of r using a log-log plot, and using a weighted least squares fit, we were able to obtain the slope, whose reciprocal equals the value of ν. Figure 6 shows one such plot, for 3D. In contrast, using Eq. (2), our data was not sufficient to obtain the value of ν, not even for a better value for p_c. It seems that more and larger samples are needed to accurately use this relation.

In Fig. 6 we compared our results with the expected behavior that follows the well established [2] value of ν in 3D (ν=0.88). In fact, the value we obtained from the slope, ν =0.77±0.13, appears to be a rather poor estimate of the well established value. As such, the relatively few simulations we used in the continuum do not appear to yield values that can be compared with values found by many more simulations on lattices [1,2,49]. However, repeating the same procedure for all other dimensions yields the well known trend of the dimensionality dependence of ν. To see this we plotted all the ν values that we derived, with their confidence limits, in Fig. 7, and compared them with those derived for lattices. The solid curve connects the values of ν as given by Fisch and Harris [49], using a weighted average of available data as obtained by several methods (mean cluster size, renormalization, finite-size scaling). The dotted line for $d \geqslant 6$ refers to the mean field value of $\nu=1/2$ for dimensions greater than six, the upper critical dimension for percolation [1,2]. We see that our results all lie below the expected curve, and as such can serve at least as lower bounds for the true ν values. It further appears that, although obtained by modestly sized samples, our results can serve for semiquantitative estimates of percolation properties. It is of course expected that with the increase of the number of simulations, the results obtained will approach those given by the accurate lattice simulations. At this stage it is encouraging to find out that for the rather few simulations that we ran, the values we obtained for ν are only 10–20 % lower than the expected values. Furthermore, we can conclude that the approach of the critical exponents in the continuum towards the true values is, from below, as one would expect from finite size effects. On the one hand, our results show that one can estimate critical parameters from and for continuum systems by simulations, and on the other hand, that results, such as the one derived in Fig. 6, can be useful if evaluated when the corresponding trend and estimates of the accuracy are given.

To summarize, we have shown that the results we have obtained for the thresholds in the continuum are consistent with finite-size scaling. This consistency expresses itself not only qualitatively, in that the statistics improve and the threshold is lower for larger samples, but also semiquantitatively, in that one can obtain the critical exponent ν from these trends.

V. SUMMARY AND DISCUSSION

In this work we have defined and described the continuum percolation thresholds in low and high dimensions. We have related these thresholds to the lattice thresholds, and introduced various invariant quantities and have computed their values.

In order to further extend the study of the thresholds in the continuum, both qualitatively and quantitatively, to high dimensions, we have used highly efficient algorithms which allowed us to accurately compute continuum thresholds for larger systems. By performing simulations on many samples, we have seen how the percolation threshold varies with the object shape (including aspect ratio, for a given shape), system dimension and sample size. From the dependence of the threshold statistics on sample size, we have succeeded in confirming the connection with the system correlation length and its critical exponent.

We have shown the role played by the excluded volume, as opposed to the volume, in continuum percolation. In fact, for randomly-aligned elongated objects, one can thus explain the near-zero thresholds [50] seemingly obtained in certain continuum systems. We have also successfully compared our results to the theory for the cases that apply, filling up the gap of the inability of the available theories to predict continuum thresholds for all the above cases.

Several general trends can be seen from our results: the percolation threshold decreases with system dimension, as expected, but the new observation is that the type of decrease is very sensitive to the object's shape in the system. Specifically, for hyperspheres we get the counterintuitive result that $B_c < 1$ for $d \geqslant 12$ (which is also true for V_{ex} of lattices [19] for $d \geqslant 4$), while for hypercubes B_c approaches an asymptotic limit with a B_c that appears to be larger than 1. Apparently, at higher dimensions the difference between the behavior of systems of these two objects gets greatly exaggerated, causing a drastically different behavior. Similarly, the thresholds of 3D boxes decrease with increasing aspect ratio in a manner similar to the decrease of hypercube thresholds with increasing dimension.

We have explained the fact that the thresholds for hyperspheres are lower than for hypercubes in very high dimensions, while the opposite is true at lower dimensions, by comparing the volume of a hypersphere, $V_{\bigcirc}$, with the volume of an "effectively equivalent" hypercube, $V_{\square}$, and looking at $V_{ratio} = V_{\bigcirc}/V_{\square}$.

We have observed that the continuum thresholds (in terms of V_{ex} and B_c) are higher than the lattice thresholds at low dimensions, apparently since they interpenetrate and pack less efficiently. At high dimensions, however, this effect is reversed for lattice bond percolation B_c (but not for lattice site percolation V_{ex}).

A comparison of the high-dimensional trends of the continuum and lattice thresholds shows the following behavior: for continuum hyperspheres, $V_{ex} = B_c \sim d^{-0.8}$ with $B_c < 1$ at high dimensions ($d \geqslant 12$); for lattice bond percolation, B_c levels off at 1 and roughly follows the $d/(d-1)$ rule; for lattice site percolation, V_{ex} goes down strongly with dimension and $V_{ex} < 1$ already at $d \geqslant 4$. Perhaps this has to do with the fact that in lattices $V \sim r^d$ for a given radius, while the number of bonds $B \sim d$ (i.e., the coordination number is proportional to the dimension). Since V is more dependent on dimension than B, V_{ex} changes more drastically with dimension than B_c. But for the continuum the number of bonds is not limited by the lattice structure and $V_{ex} = B_c$.

The study of continuum thresholds is a rich and diverse topic, and we have studied only a few types of systems described by continuum percolation theory. Thus, continuum systems of objects with size or shape distribution [28], with hard-core exclusion [46,51], or with interparticle interaction [52], have not been dealt with here. We have attempted, however, to focus on specific trends, in particular for higher dimensions [22], and thus shed some light on the entire continuum percolation threshold problem.

APPENDIX: EXCLUDED VOLUME OF BOXES

A box of aspect ratio a in d dimensions has a volume $v = ae^d$, where e is the length of the short edges, and (ae) is the length of the single long edge.

To compute the average excluded volume, we consider here only systems of boxes that are parallel or perpendicular to each other. Two boxes may then intersect in two different situations: when their long edges are parallel (i.e., lie along the same axis), or where their long edges are perpendicular (i.e., lie along different axes).

For the parallel case, the volume around the center of one box, into which a second box may not enter without intersecting the first, V_m, is clearly given by $V_m = a(2e)^d = 2^d ae^d = 2^d v$.

For the perpendicular case, we compute the excluded volume V_n by "moving" the second box around the first. The volume described by this "movement" has two edges of length $(ae+e)$, and all the other edges of length $(e+e)$. Hence

$$\begin{aligned} V_n &= (ae+e)^2(2e)^{d-2} \\ &= (a+1)^2 e^2 2^{d-2} e^{d-2} \\ &= (a+1)^2 2^{d-2} e^d \\ &= [(a+1)^2/4a] 2^d ae^d \\ &= [(a+1)^2/4a] 2^d v. \end{aligned}$$

To compute $\langle V \rangle$, the average excluded volume for a given box, we must average over these two possibilities. For a randomly-aligned system with an isotropic distribution, a second box intersects a first box, in any given position, with probability $1/d$ for a parallel intersection, and probability $(d-1)/d$ for perpendicular intersection. Hence

$$\begin{aligned} \langle V \rangle &= [1/d] V_m + [(d-1)/d] V_n \\ &= [2^d/d] v + [(d-1)/d][(a+1)^2/4a] 2^d v \\ &= [2^d v/d][1 + (d-1)(a+1)^2/4a]. \end{aligned}$$

We note that for $a=1$, $\langle V \rangle$ simply reduces to $2^d v$, which is the case of hypercubes.

For boxes with large aspect ratios ($a \gg 1$) we see that $V_m \ll V_n$. Hence,

$$\begin{aligned} \langle V \rangle &= [(d-1)/d] V \\ &= [(d-1)/d][(a+1)^2/4a] 2^d v \\ &= [(d-1)/d] 2^{d-2} a^2 e^d. \end{aligned}$$

For the 3D boxes discussed in this work, this reduces of course to $\langle V \rangle = (4/3) a^2 e^3$.

[1] R. Zallen, *The Physics of Amorphous Solids* (Wiley, New York, 1983).

[2] D. Stauffer and A. Aharony, *Introduction to Percolation Theory* (Taylor and Francis, London, 1994).

[3] *Fractals and Disordered Systems*, 2nd edition, edited by A. Bunde and S. Havlin (Springer, Berlin, 1996), and references therein.

[4] M. Sahimi, in *The Mathematics and Physics of Disordered Media—Lecture Notes in Mathematics No. 1035*, edited by B. D. Hughes and B. W. Ninham (Springer, Berlin, 1983), p. 314.

[5] S. Kirkpatrick, in Les Houches XXI—*Ill-Condensed Matter*, edited by R. Balian, R. Maynard, and G. Toulouse (North-Holland, Amsterdam, 1979), p 321.

[6] S. Feng, B. I. Halperin, and P. N. Sen, Phys. Rev. B **35**, 197 (1987).

[7] P. M. Kogut and J. Straley, J. Phys. C **12**, 2151 (1979); P. N. Sen, J. N. Roberts, and B. I. Halperin, Phys. Rev. B **32**, 3306 (1985); M. Murat, S. Mariner, and D. J. Bergman, J. Phys. A **19**, L275 (1986); A. Bunde, H. Harder, and S. Havlin, Phys. Rev. B **34**, 3540 (1986).

[8] See for example, D. Ben-Avraham and S. Havlin, *Diffusion and Reactions in Fractals and Disordered Systems* (Cambridge Univ. Press, Cambridge, 2000); M. Sahimi, *Applications of Percolation Theory* (Taylor and Francis, London, 1994).

[9] R. F. Voss, R. B. Laibowitz, and E. I. Alessandrini, Phys. Rev. Lett. **49**, 1441 (1982); A. Kapitulnik and G. Deutscher, *ibid.* **49**, 1444 (1982).

[10] C. H. Seager and G. E. Pike, Phys. Rev. B **10**, 1435 (1974).

[11] D. J. Bergman, Phys. Rev. B **33**, 2013 (1986).

[12] D. Stauffer, A. Coniglio, and M. Adam, Adv. Polym. Sci. **44**, 1103 (1982).

[13] G. E. Pike and C. H. Seager, Phys. Rev. B **10**, 1421 (1974), T. Vicsek and J. Kertesz, J. Phys. A **14**, L31 (1981), E. T. Gawlinski and H. E. Stanley, J. Phys. A **14**, L291 (1981), and J. Kertesz and T. Vicesk, Z. Phys. B: Condens. Matter **45**, 345 (1982); W. T. Elam, A. R. Kerstein, and J. J. Rehr, Phys. Rev. Lett. **52**, 1516 (1984).

[14] V. K. S. Shante and S. Kirkpatrick, Adv. Phys. **20**, 325 (1971).

[15] A. Coniglio, U. De Angelis, A. Forliani, and G. Lauro, J. Phys. A **10**, 219 (1977); A. Coniglio, U. De Angelis, and A. Forliani, *ibid.* **10**, 1123 (1977).

[16] A. L. R. Bug, S. A. Safran, and I. Webman, Phys. Rev. Lett. **54**, 1412 (1985).

[17] O. Stenull and H-K. Janssen, Phys. Rev. E **68**, 036129 (2003).

[18] G. Paul, R. M. Ziff, and H. E. Stanley, Phys. Rev. E **64**, 0261115 (2001).

[19] P. Grassberger, Phys. Rev. E **67**, 036101 (2003).

[20] H. Nakanishi and H. E. Stanley, Phys. Rev. B **22**, 2466 (1980).

[21] H-P. Hsu, W. Nadler, and P. Grassberger, J. Phys. A **38**, 775 (2005).

[22] S. Fortunato, D. Stauffer, and A. Coniglio, Physica A **334**, 307 (2004).

[23] J. F. McCarthy, Phys. Rev. Lett. **58**, 2242 (1987).

[24] V. A. Vyssotsky, S. B. Gordon, H. L. Frisch, and J. M. Hammersley, Phys. Rev. **123**, 1566 (1961).

[25] N. W. Dalton, C. Domb, and M. F. Sykes, Proc. Phys. Soc. London **83**, 496 (1964).

[26] H. Scher and R. Zallen, J. Chem. Phys. **53**, 3759 (1970).

[27] P. C. Robinson, J. Phys. A **16**, 605 (1983); I. Balberg and N. Binenbaum, Phys. Rev. B **28**, 3799 (1983).

[28] I. Balberg, C. H. Anderson, S. Alexander, and N. Wagner, Phys. Rev. B **30**, 3933 (1984).

[29] L. Onsager, Ann. N.Y. Acad. Sci. **51**, 627 (1949).

[30] I. Balberg, N. Binenbaum, and N. Wagner, Phys. Rev. Lett. **52**, 1465 (1984).

[31] Z. Neda, R. Florian, and Y. Brechet, Phys. Rev. E **59**, 3717 (1999).

[32] E. Charlaix, J. Phys. A **19**, L533 (1986).

[33] E. Charlaix, E. Guyon, and N. Rivier, Solid State Commun. **50**, 999 (1984).

[34] I. Balberg, Phys. Rev. B **31**, 4053 (1985).

[35] T. L. Hill, *Statistical Mechanics* (McGraw Hill, New York, 1956).

[36] T. de Simone, S. Demoulini, and R. M. Stratt, J. Chem. Phys. **85**, 391 (1986).

[37] U. Alon, A. Drory, and I. Balberg, Phys. Rev. A **42**, 4634 (1990).

[38] A. Drory, I. Balberg, U. Alon, and B. Berkowitz, Phys. Rev. A **43**, 6604 (1991). For a review, see A. Drory and I. Balberg, in *Trends in Statistical Physics*, edited by B. Chirikov, A. De Masi, J. Fritz, S. Havlin, V. Privman, and H. Spohn (Research Trends, Poojapora, 2000), Vol. 3, p. 45.

[39] N. Wagner, D. Klein, and I. Balberg (unpublished).

[40] N. Wagner and I. Balberg, J. Stat. Phys. **49**, 369 (1987).

[41] J. Hoshen and R. Kopelman, Phys. Rev. B **14**, 3438 (1976).

[42] M. D. Rintoul and S. Torquato, J. Phys. A **30**, L585 (1997).

[43] E. T. Gawlinski and S. Redner, J. Phys. A **16**, 1063 (1983).

[44] D. R. Baker, G. Paul, S. Sreenivasan, and H. E. Stanley, Phys. Rev. E **66**, 046136 (2002).

[45] S. W. Haan and R. Zwanzig, J. Phys. A **10**, 1547 (1977).

[46] U. Alon, I. Balberg, and A. Drory, Phys. Rev. Lett. **66**, 2879 (1991), and unpublished results.

[47] S. Kirkpatrick, Phys. Rev. Lett. **36**, 69 (1976).

[48] M. E. Levinshtein, B. I. Shklovskii, M. S. Sur, and A. L. Efros, Sov. Phys. JETP **42**, 197 (1976); B. I. Shklovskii and A. L. Efros, *Electronic Properties of Doped Semiconductors* (Springer-Verlag, Berlin, 1984).

[49] R. Fisch and A. B. Harris, Phys. Rev. B **18**, 416 (1978).

[50] I. Balberg, Phys. Rev. B **33**, 3618 (1986).

[51] A. Drory, I. Balberg, and B. Berkowitz, Phys. Rev. E **49**, R949 (1994).

[52] A. L. R. Bug, S. A. Safran, G. S. Grest, and I. Webman, Phys. Rev. Lett. **55**, 1896 (1985).